Interaction of Al 2 O 3 and CeO 2 Surfaces with SO 2 and SO 2 + O 2 Studied by X-ray Photoelectron Spectroscopy

ARTICLE *in* THE JOURNAL OF PHYSICAL CHEMISTRY B · JUNE 2005

Impact Factor: 3.3 · DOI: 10.1021/jp0508249 · Source: PubMed

7 AUTHORS, INCLUDING:

Mikhail Yu. Smirnov
Boreskov Institute of Catalysis
48 PUBLICATIONS **494** CITATIONS
SEE PROFILE

Alexei Sorokin
Boreskov Institute of Catalysis
16 PUBLICATIONS **202** CITATIONS
SEE PROFILE

Valerii Bukhtiyarov
Boreskov Institute of Catalysis
184 PUBLICATIONS **2,656** CITATIONS
SEE PROFILE

Interaction of Al_2O_3 and CeO_2 Surfaces with SO_2 and $SO_2 + O_2$ Studied by X-ray Photoelectron Spectroscopy

Mikhail Yu. Smirnov,* Alexander V. Kalinkin, Andrei V. Pashis, Alexei M. Sorokin, Alexander S. Noskov, Karl C. Kharas,† and Valerii I. Bukhtiyarov

Boreskov Institute of Catalysis SB RAS, Lavrentieva ave, 5, Novosibirsk 630090, Russia, and Delphi, Tulsa, Oklahoma 74158-0970

Received: February 16, 2005; In Final Form: April 22, 2005

The interaction of Al_2O_3 and CeO_2 thin films with sulfur dioxide (2.5 mbar) or with mixtures of SO_2 with O_2 (5 mbar) at various temperatures (30−400 °C) was studied by X-ray photoelectron spectroscopy (XPS). The analysis of temperature-induced transformations of S2p spectra allowed us to identify sulfite and sulfate species and determine the conditions of their formation on the oxide surfaces. Sulfite ions, SO_3^{2-}, which are characterized by the $S2p_{3/2}$ binding energy (BE) of ∼167.5 eV, were shown to be formed during the interaction of the oxide films with pure SO_2 at temperatures ≤200 °C, whereas sulfate ions, SO_4^{2-}, with BE ($S2p_{3/2}$) ∼169 eV were produced at temperatures ≥300 °C. The formation of both the sulfite and sulfate species proceeds more efficiently in the case of CeO_2. The addition of oxygen to SO_2 suppresses the formation of the sulfite species on both oxides and facilitates the formation of the sulfate species. Again, this enhancement is more significant for the CeO_2 film than for the Al_2O_3 one. The sulfation of the CeO_2 film is accompanied by a reduction of Ce(IV) ions to Ce(III) ones, both in the absence and in the presence of oxygen. It has been concluded that the amount of the sulfates on the CeO_2 surface treated with the $SO_2 + O_2$ mixture at ≥300 °C corresponds to the formation of a 3D phase of the Ce(III) sulfate. The sulfation of Al_2O_3 is limited by the surface of the oxide film.

1. Introduction

Studying the interaction of SO_2 with surfaces of alumina and ceria is of importance, first of all, because of their catalytic application. High surface area Al_2O_3 is used as a catalyst for the Claus process in which SO_2 is reduced to sulfur by hydrogen sulfide. Furthermore, both Al_2O_3 and CeO_2 are the main components of monolith catalysts for the purification of exhaust gases emitted from car engines. Sulfur dioxide, which is one of the pollutants released to the atmosphere as a result of fuel combustion, can react with components of the emission control catalysts, reducing the activity of the catalysts in CO, NO_x, and hydrocarbon abatement.[1] Therefore, the interaction of SO_2 with Al_2O_3 and CeO_2 surfaces has been studied widely in the past.[2−25] However, the results of these investigations are often contradictory. These contradictions concern, first of all, the nature and properties of reaction products and, second, the conditions of their appearance.

It has been shown that the adsorption of SO_2 on Al_2O_3 surfaces in a wide range of temperatures (−100 to 500 °C) and partial pressures of ≥10 mbar results in the formation of several weakly and strongly bonded species, which, on the basis of infrared (IR) spectra, have been identified as sulfite species SO_3^{2-}.[2−8] It has been established that the sulfite species are adsorbed on basic sites,[4] which, for instance, can be terminal O^{2-} ions on the alumina surface. It has been found that the higher the strength of the Lewis basicity of an oxide the greater the amount of SO_2 strongly held in the form of sulfite species.[7−10] The sulfite species were found to decompose completely after annealing the sample in vacuum at temperatures of 600 °C and above.[2,3,5] The oxidation of the sulfite species with oxygen or the treatment of alumina with $SO_2 + O_2$ mixtures at $T \approx 400-700$ °C have been shown to result in the formation of sulfate species.[2,3,6,8,11−14] In contrast, a concurrent formation of the sulfite and sulfate species on γ-Al_2O_3 after its interaction with SO_2 at 80 °C was reported on the basis of X-ray photoelectron spectroscopy (XPS) data.[15] The amounts of the sulfite and sulfate species produced under the interaction of SO_2 or $SO_2 + O_2$ with alumina did not exceed 2×10^{14} cm^{-2},[7,10,13,16] that is, the interaction with Al_2O_3 was most probably limited only by the surface area. Different structures with various types of coordination have been proposed for sulfite and sulfate species on the surface of Al_2O_3.[11,12,17−19]

The interaction of SO_2 with CeO_2 at elevated temperatures and the mbar SO_2 partial pressure range has also been studied extensively.[10,20−22] As concluded from gravimetric[22] and elemental analysis[10] measurements, the accumulation of sulfur species occurs mainly in the form of sulfite and hydrosulfite and does not exceed $\sim 5 \times 10^{14}$ S atoms per cm^2, when the adsorption proceeds in the temperature range of 30−350 °C. According to an IRS study,[22] the treatment of sulfite in a large excess of oxygen at 400 °C leads to the formation of both surface and bulk sulfates. The heating of the sulfated ceria up to 600 °C results in decomposition of the bulk sulfate, whereas the surface sulfate persists even at 700 °C.[22] At the same time, XPS studies performed in UHV have revealed that sulfite and even sulfate species were produced under SO_2 adsorption on a CeO_2 film at room temperature or below.[23−25] The total amount of the sulfite and sulfate species accumulated did not exceed a monolayer (ML) after a dose of SO_2 in 5 L (1 L (Langmuir) = 1.3×10^{-6} mbar × sec) and became larger than 1 ML after treatment in 1.7 mbar of SO_2 at 30 °C for 5 min.[24] It has been

* Corresponding author. E-mail: smirnov@catalysis.nsk.su.
† Delphi.

10.1021/jp0508249 CCC: $30.25
Published on Web 05/20/2005

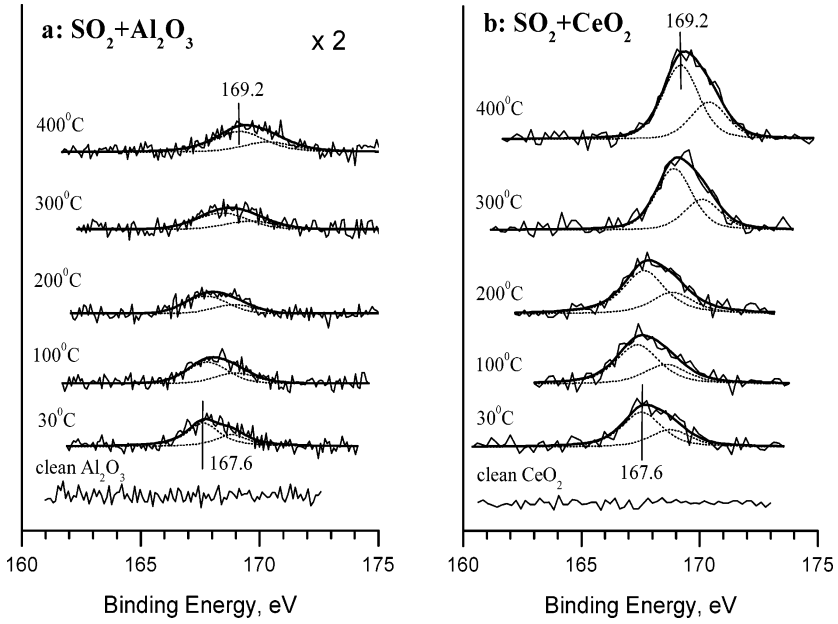

Figure 1. The S2p photoemission spectra recorded after the treatment of the alumina (a) and ceria (b) films in 2.5 mbar SO_2 for 20 min at the temperatures indicated. For the case of Al_2O_3, the spectra are multiplied by factor 2.

concluded that the interaction of SO_2 with CeO_2 does not change the oxidation state of cerium Ce(IV), and, therefore, the formation of SO_4^{2-} was assumed to take place via disproportionation of SO_2 into Ce(IV) sulfate and SO.[24] In contrast, sulfate formation detected by XPS/TPD measurements under treatment of a CeO_2 film in mixture $SO_2 + O_2$ (1:1) at total pressure of 8×10^{-5} mbar and 25 °C was accompanied by partial reduction of Ce(IV) into Ce(III).[25] The sulfite species have a moderate thermal stability and decompose releasing $SO_{2,g}$ in the temperature range from −70 to 330 °C. The temperature interval of the sulfate species decomposition determined in different works varies from −70 to 330 °C[24] to 530−730 °C.[25]

As evidenced by the foregoing survey, the results obtained in UHV and in the millibar pressure range led to the conflicting conclusions concerning the nature of the products and their thermal stability. One can suggest that these contradictions are most probably determined by the effect of temperature, pressure, and the content of the gas phase on the chemical nature of sulfur-containing species produced during reactions of SO_2 with Al_2O_3 or with CeO_2. To bridge the UHV and real catalytic conditions and to obtain more information about the sulfation mechanisms of oxide surfaces, a comparative XPS study of the interaction of SO_2 and $SO_2 + O_2$ with Al_2O_3 and CeO_2 was undertaken in this work.

2. Experimental Section

All of the experiments were performed using a VG ESCA 3 spectrometer with the base pressure $<5 \times 10^{-9}$ mbar. X-ray photoelectron spectra were taken using nonmonochromatized Al Kα irradiation ($h\nu = 1486.6$ eV). Before taking measurements, we calibrated the spectrometer against the $Au4f_{7/2}$ binding energy (BE) of 84.0 eV and the $Cu2p_{3/2}$ BE of 932.6 eV. The original data acquisition system was used for XPS signal detection and control of the sample temperature.[26]

A thin film of Al_2O_3 was prepared via evaporation of metallic aluminum in the presence of oxygen ($P(O_2) = 10^{-4}$ mbar) on a clean surface of a tantalum foil. The necessary thickness of the alumina film was achieved via a number of repetitive evaporation cycles and was larger than ∼100 Å. This estimation was based on the complete disappearance of the tantalum lines from XPS spectra. Finally, the alumina foil was annealed for 10 min at $P(O_2) = 10^{-4}$ mbar and $T = 600$ °C. Afterward, the binding energies and intensity ratio of Al2p and O1s lines were found to correspond to the Al_2O_3 composition.

A thin film of CeO_2 was obtained via subsequent UHV evaporation of metallic cerium over the Al_2O_3 film followed by oxidation at $P(O_2) = 2.5 \times 10^{-5}$ mbar and $T = 600$ °C. The role of the intermediate alumina film was to prevent diffusion of very mobile oxygen from cerium oxide into the tantalum foil, thereby maintaining the stoichiometry of the CeO_2 film. As a consequence, Ce3d, Ce4d, and O1s lines taken from the film were typical of CeO_2. Again, repetitive evaporation cycles were applied to produce the desirable thickness of the ceria films. Based on the attenuation of the Al2p intensity, the thickness of the CeO_2 film was estimated at about 20−30 Å.

The treatments in SO_2 (2.5 mbar) or $SO_2 + O_2$ (2.5 mbar + 2.5 mbar) were performed in a preparation chamber of the spectrometer for 20 min at various temperatures: 30, 100, 200, 300, and 400 °C. The sample was heated resistively by passing a current through the tantalum foil. The temperature of the sample was measured with a chromel−alumel thermocouple spot-welded to the Ta foil. After cooling to room temperature and evacuation of the reaction mixture, the sample was transferred into the analyzer chamber, where survey XP spectra as well as narrow spectra of Al2p, S2p, O1s, and Ce3d regions were measured. The binding energies and intensities were calculated after subtraction of a Shirley-type background from raw photoemission spectra. Complex spectra in the Ce3d region were resolved into eight components: six for the Ce(IV) and two for the Ce(III) oxidation states (see below), according to a fitting procedure described elsewhere.[27] The BE (Al2p) = 74.5 eV and BE (Ce3d u''') = 916.7 eV were used as references for the cases of Al_2O_3 and CeO_2, respectively.[27,28] The atomic ratios of S/Al and S/Ce were calculated from S2p, Al2p, and Ce3d areas using the corresponding atomic sensitivity factors (ASF) taken in.[29]

3. Results

Figure 1 presents two sets of S2p spectra taken from Al_2O_3 (a) and CeO_2 (b) films after their interaction with sulfur dioxide

TABLE 1: Values of $S2p_{3/2}$ BE for Various Sulfur-Containing Compounds and Adsorbed Species

	sulfides		sulfur		sulfites		sulfates	
	Na_2S	PtS	S	Na_2SO_3	$PbSO_3$	Na_2SO_4	$PbSO_4$	$Fe_2(SO_4)_3$
BE, eV	161.8	163.6	~164	166.5	167.8	168.7	169.4	169.1
ref	30	31	30, 32	30	33	30	33	30

TABLE 2: $S2p_{3/2}$ Binding Energies and S/Al and S/Ce Atomic Ratios Measured after the Treatment of Al_2O_3 and CeO_2 with SO_2 at Various Temperatures

	BE, eV		S/Al and S/Ce atomic ratios	
temperature, °C	Al_2O_3	CeO_2	Al_2O_3	CeO_2
30	167.6	167.6	0.041	0.13
100	167.8	167.4	0.038	0.18
200	167.7	167.7	0.032	0.19
300	168.4	168.9	0.032	0.19
400	169.2	169.2	0.046	0.22

TABLE 3: $S2p_{3/2}$ Binding Energies and S/Al and S/Ce Atomic Ratios Measured after the Treatment of Al_2O_3 and CeO_2 with $SO_2 + O_2$ at Various Temperatures

	BE, eV		S/Al and S/Ce atomic ratios	
temperature, °C	Al_2O_3	CeO_2	Al_2O_3	CeO_2
30	168.6	167.7	0.012	0.063
100	168.6	168.1	0.017	0.072
200	168.6	168.9	0.016	0.19
300	169.2	169.1	0.036	0.29
400	169.2	169.1	0.060	0.45

(see Experimental Section) at various temperatures. One can see that the treatment of the oxides by SO_2 results in an appearance of S2p features, both their intensities and positions being dependent on temperature. The asymmetrical shape of the features is explained by the spin−orbital splitting of the S2p spectrum on two components, $S2p_{3/2}$ and $S2p_{1/2}$. To analyze these spectra in more detail and to apply literature data for comparison, we deconvoluted the S2p lines into these components. As seen from Table 1, which lists literature data for various sulfur-containing compounds, namely, the $S2p_{3/2}$, binding energies were usually applied to elucidate the chemical state of sulfur. Despite a structureless shape of the S2p spectra, such deconvolution is straightforward because both the spin−orbital splitting of 1.2 eV and the component ratio $S2p_{3/2}/S2p_{1/2} = 2:1$ are well known from previous papers, which have applied synchrotron radiation as a source of X-rays.[24]

The $S2p_{3/2}$ binding energies as well as the S/Al and S/Ce atomic ratios determined from the spectra of Figure 1 are collected in Table 2. One can see that similar behaviors of the S2p spectra are observed for both oxides. Being located at 167.5 ± 0.2 eV at temperatures below 200 °C, the $S2p_{3/2}$ features are shifted to higher BE as the sample temperature rises to 300 °C and achieve the BE value of 169.2 eV at 400 °C (Figure 1, Table 2). The comparison with literature data (Table 1) allows unambiguous assignment of these $S2p_{3/2}$ features to sulfite (~167.5 eV) and sulfate (~169.2 eV) species. The data presented in Table 2 also show that the CeO_2 surface contains a higher amount of sulfur-containing species in both temperature ranges. Furthermore, the abundance of sulfur on the Al_2O_3 surface is weakly dependent on the reaction temperature, whereas for CeO_2, the abundance of sulfur has a tendency to increase with the reaction temperature.

The $S2p_{3/2}$ spectra taken from the Al_2O_3 (a) and CeO_2 (b) surfaces after their interaction with $SO_2 + O_2$ mixtures at various temperatures are shown in Figure 2. A comparison of the spectra in Figures 1 and 2 indicates that the addition of O_2 to an SO_2 flow changes the composition of the overlayers. This conclusion also follows from the data of Table 3, which shows $S2p_{3/2}$ binding energies and S/Al, S/Ce atomic ratios determined from the spectra of Figure 2. First of all, suppression of the sulfite formation for both oxides at $T < 200$ °C should be mentioned. One can see that the intensity of the S2p spectra measured from the Al_2O_3 surface at $T \leq 200$ °C is comparable with the XPS sensitivity limit (Figure 2a). Higher values of the $S2p_{3/2}$ binding energies registered in this temperature range, 168.6 eV (Table 3), compared to those typical of sulfite (167.5−167.7 eV) is another difference of the $SO_2 + O_2$ mixture treatment. This shift can be explained by the formation of the sulfate ions admixed with the sulfite species. Unfortunately, the low intensity of S2p signals does not allow us to carry out a more detailed analysis of these spectra. Similar to the alumina surface, the interaction of CeO_2 with the $SO_2 + O_2$ mixture decreases the amount of sulfite produced at room temperature and shifts the sulfite-originated S2p feature to higher binding energies at 100 °C (Figure 2b and Table 3). The complete transformation of the sulfite overlayer to the sulfate one at 200 °C seems to prove that the intermediate position of the S2p spectra at lower temperatures originates from coadsorption of the sulfite- and sulfate-originated features.

A more pronounced accumulation of the sulfates at $T >$ 200 °C (Figure 2b, Table 3) is another result of the O_2 influence on the SO_2 interaction with the alumina and ceria surfaces. One can see that for both oxides, the sulfate yield enhances with the reaction temperature (Tables 2 and 3). It is also noteworthy that efficient sulfate formation on the ceria film occurs at a temperature about 100 °C below that of the reaction with pure SO_2.

Figure 3 compares the yields of the sulfate species produced in the reactions of the Al_2O_3 and CeO_2 with SO_2 and $SO_2 + O_2$ at various temperatures. The sulfate yields were expressed as S/Al and S/Ce atomic ratios calculated from the intensities of the corresponding photoemission lines. One can see that the formation of the sulfate species occurs more efficiently on the CeO_2 film. The diagrams in Figure 3 also show that the efficiency of sulfation increases with temperature. In the presence of oxygen, the sulfation emerges at a lower temperature and proceeds with a larger yield of sulfate species. The influence of oxygen and temperature on the sulfation is more pronounced in the case of CeO_2.

An essential difference in the sulfation of Al_2O_3 and CeO_2 is also exhibited in the behavior of the Al2p and Ce3d lines. The parameters of the Al2p line change negligibly under the reaction, indicating the permanency in the chemical state of aluminum ions. Contrary to alumina, a part of the Ce(IV) ions transform into the Ce(III) ions as a result of the interaction of the CeO_2 surface with pure SO_2 or with the $SO_2 + O_2$ mixture. This conclusion is based on the data of Figure 4, which demonstrates the variation of the Ce3d spectra after the treatment of CeO_2 with SO_2 (a) or with $SO_2 + O_2$ (b) at various temperatures. The Ce3d spectra of the initial CeO_2 surfaces are also shown for comparison.

As mentioned in the Experimental Section, the Ce3d spectra have a complex structure composed of three $Ce3d_{5/2}/Ce3d_{3/2}$ doublets from Ce(IV) ions and one doublet from Ce(III) ones.[27,28,34] The $Ce3d_{5/2}$ lines, characteristic of the Ce(IV) oxidation state, are located at 882.4, 889.0, and 898.3 eV. Following convention,[27,28] these features are designated as v, v'', and v'''. The corresponding u, u'', and u''' features of the $Ce3d_{3/2}$ lines appear at 900.8, 907.4, and 916.7 eV. This

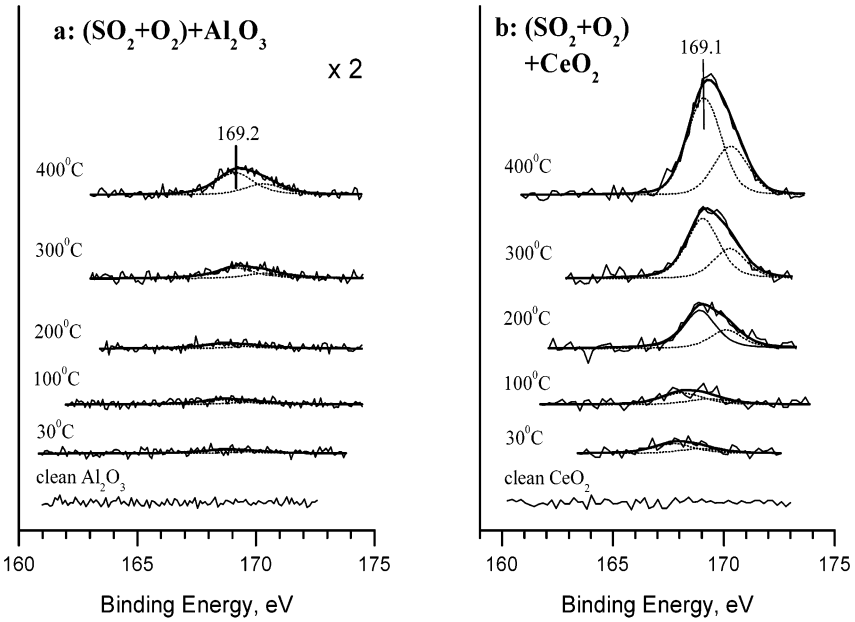

Figure 2. The S2p photoemission spectra recorded after the treatment of the alumina (a) and ceria (b) films in 2.5 mbar SO_2 + 2.5 mbar O_2 for 20 min at the temperatures indicated. For the case of Al_2O_3, the spectra are multiplied by factor 2.

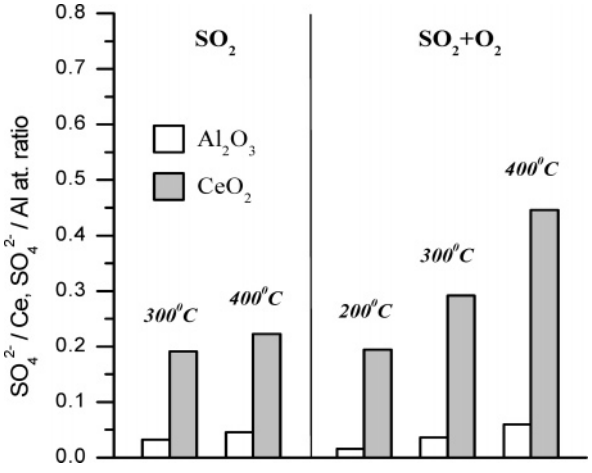

Figure 3. The S/Al and S/Ce atomic ratios calculated for the sulfate species produced on the alumina and ceria films treated in 2.5 mbar SO_2 or the mixture of 2.5 mbar SO_2 and 2.5 mbar O_2 at the temperatures indicated.

complicated structure of the Ce3d spectrum is determined by the electronic structure of cerium ions in the initial and final states. As a result of a strong hybridization between the Ce^{4+} and O^{2-} valence orbitals, the initial electronic state of cerium ions in CeO_2 is a mixture $4f^0$ and $4f^1L^{-1}$ configurations, where L^{-1} denotes a hole in the valence band.[34] According to literature data,[35,36] the v'''/u''' doublet corresponds to the photoionization into the $4f^0$ final state, whereas two other doublets, v''/u'' and v/u, correspond to the final state in which the $4f^1$ and $4f^2$ configurations are mixed. The $Ce3d_{5/2}/Ce3d_{3/2}$ lines at 885.6 and 904.0 eV designated in Figure 4 as v' and u' features arise from the Ce^{3+} ions.[27] In general, the spectrum of the pure Ce(III) oxidation state is characterized additionally by another doublet, designated as v_0/u_0. However, the position and intensity of these minor lines allows us to exclude them from consideration. Indeed, their addition to the v'/u' lines leads only to a slight broadening and asymmetry of the entire Ce3d spectrum from Ce(III) ions. Therefore, the contribution of the v_0/u_0 doublet into the Ce3d spectra is not taken into account in this work. As a consequence, Figure 4 shows the Ce3d spectra together with their deconvolution into the eight above-mentioned components belonging to the Ce(IV) and Ce(III) states. The fraction of Ce(III) ions in the CeO_2 films was estimated as a ratio of the total intensity of the v' and u' components to the total intensity under the entire Ce3d contour. This estimation indicated that the initial ceria films, before the treatment in SO_2-containing mixtures, comprises about 15% of Ce(III) ions. The XPS detection of the Ce(III) oxidation state in the clean and preoxidized ceria samples has been reported frequently in literature.[27,36−38] There are several reasons for the observation of Ce^{3+} ions in the initial CeO_2 sample. First, the ceria surface can be reduced under the influence of X-rays.[39] Second, because our CeO_2 films were deposited on the alumina surface, their annealing in a reducing medium (see Experimental Section) can transform the ceria/alumina interface into very stable cerium (III) aluminate $CeAlO_3$, which can be reoxidized successfully in air only at very high temperatures (>600 °C).[36−38] Finally, reactions of CeO_2 with such background gases as CO and H_2 can also cause the reduction of the Ce^{4+} ions. The detailed analysis of the reasons was not made in this work because the shape of the initial spectrum (Figure 4) was close to CeO_2 and the determined fraction of the Ce(III) oxidation state (15%) did not exceed the value reported for ceria in the literature.

Analysis of the Ce3d spectra shown in Figure 4 indicates that the CeO_2 surface is reduced during the reaction with SO_2, with the extent of the reduction being increased gradually with temperature. Addition of O_2 to the SO_2 flow enhances significantly the degree of reduction when the temperature is 300 °C or above, coinciding with the formation of the sulfate species. Moreover, the comparison of the S2p (Figures 1b and 2b) and Ce3d (Figure 4) spectra allows us to conclude that the sulfation and reduction of ceria proceed in parallel. To confirm this conclusion quantitatively, we plotted the amount of the sulfate produced under the reaction of the CeO_2 film with SO_2 + O_2 mixtures in Figure 5 as a function of the Ce(III) fraction, which has been corrected for the Ce(III) content in the original CeO_2 films. This figure reveals a linear relationship between these two parameters. An attempt to plot similar parameters for the reaction with pure SO_2 led to less obvious dependence because

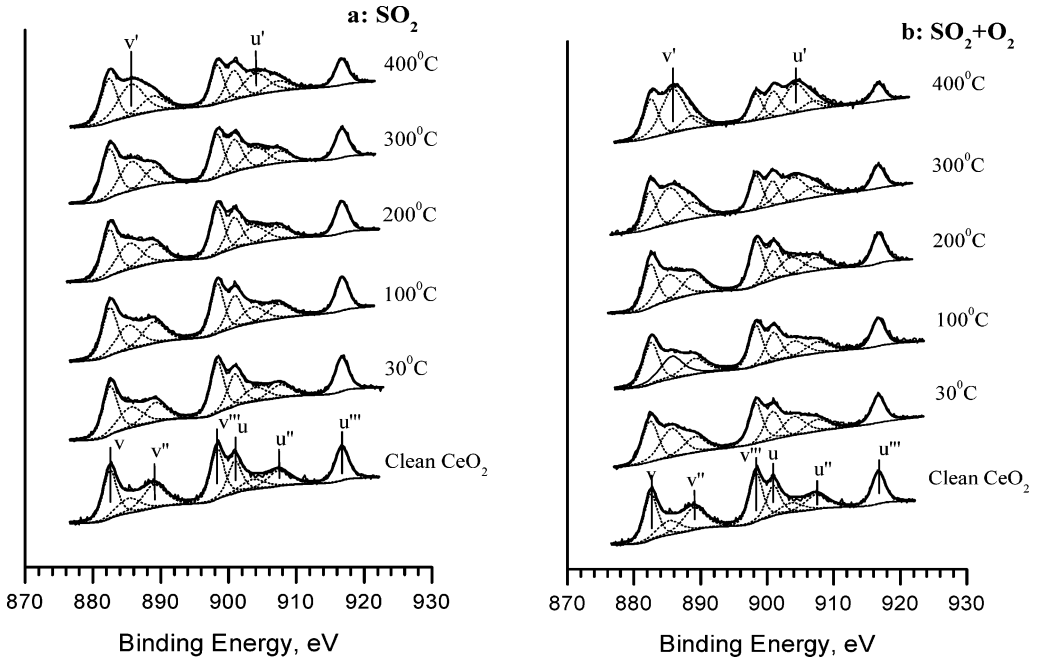

Figure 4. The Ce3d photoemission spectra recorded for the CeO_2 film treated in 2.5 mbar SO_2 (a) or 2.5 mbar SO_2 and 2.5 mbar O_2 (b) at the temperatures indicated. The bottom spectra in panels a and b characterize the initial state of the CeO_2 film before the treatments.

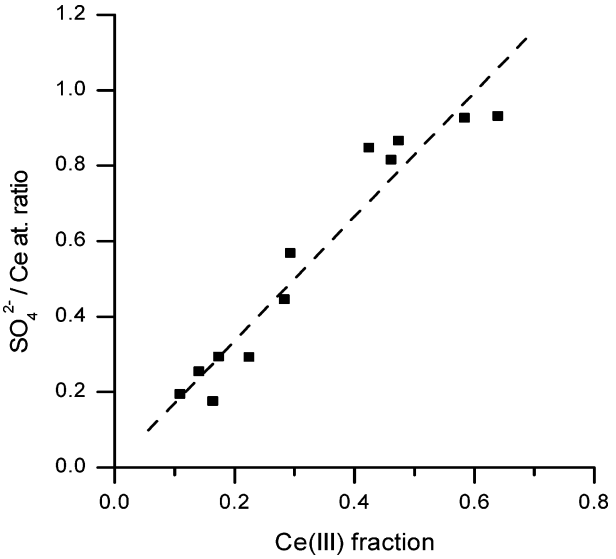

Figure 5. The yield of sulfate produced under the reaction of the CeO_2 film with 2.5 mbar SO_2 + 2.5 mbar O_2 at various temperatures as a function of the Ce(III) fraction corrected for the Ce(III) content in the initial CeO_2 film. The yield of sulfate is evaluated by the S/Ce atomic ratio.

the yield of the sulfate per one Ce(III) ion is much smaller in this case (see reactions 5 and 7 in Section 4).

4. Discussion

The systematic XPS study of the temperature-dependent adsorption of pure SO_2 and the reaction of $SO_2 + O_2$ mixtures with Al_2O_3 and CeO_2 films in the millibar pressure range provides a relatively clear picture of the transformations of the sulfur-containing species on these oxide surfaces. It has been shown unambiguously that sulfite and sulfate species are produced both in the absence and in the presence of oxygen, with their population being dependent not only on temperature but also on the nature of the oxide surfaces (Al_2O_3 or CeO_2). Differences in redox properties of nonreducible alumina and reducible ceria suggest different mechanisms of the formation of the sulfate species on these oxides.

4.1. SO_3^{2-} Formation. Sulfite-like species are the major product when pure SO_2 interacts with alumina or ceria surfaces at 200 °C or below. This conclusion is based on the appearance of the S2p features with the $S2p_{3/2}$ binding energies of ~167.6 eV that is much less than the value 169.2 eV observed at higher temperatures (Figure 1). It is obvious that the highest value of the binding energies arises from the sulfate-like species (Table 1). The most probable mechanism of the sulfite formation on an oxide surface is a molecular adsorption of SO_2 on Lewis basic sites, such as O_s^{2-} surface anions,[4] via the following surface reaction:

$$SO_2 + O_s^{2-} \rightarrow SO_3^{2-} \quad (1)$$

However, our study contains some experimental results that cannot be rationalized in the terms of this simple model. Among them are the much lower amount of the sulfite species on the Al_2O_3 surface as compared with the CeO_2 surface (Table 2) and the suppression of the sulfite formation under the influence of O_2 (Table 3). A more detailed analysis of the literature allows us to propose some reasonable explanations of these facts.

First of all, it should be taken into account that according to literature, adsorbed SO_2 on the surfaces of oxides can exist in more than one state. Even in 1978, Chang characterized two species formed on the γ-alumina surface at room temperature by IR bands at 1060 cm^{-1} and 1326−1140 cm^{-1}.[2] Karge and Dalla Lana showed by selective poisoning with Lewis acid BF_3 that the first species, called sulfite species, were chemisorbed on O^{2-} basic sites.[4] They also revealed that the IR bands at 1330−1150 cm^{-1} were blocked by water or ammonia during preadsorption. The authors have concluded that these species represent a physisorbed form of SO_2 weakly bonded to Lewis acid sites (coordinatively unsaturated aluminum ions). The amount of the weakly bonded $SO_{2,ads}$ at $T \leq 150$ °C was several times higher than the concentration of the strongly bonded species.[8] Lavalley et al. also suggested the occurrence of bisulfite species resulting from the interaction between SO_2 and the most basic OH groups of alumina.[9]

This consideration indicates that the relative population of the surface by these species should depend on the termination (Al or O ions) and degree of hydroxylation of the alumina surface under study. The formation of weakly bonded $SO_{2,ads}$ requires the presence of anion vacancies on the alumina surfaces, whereas the amount of strongly bonded $SO_{2,ads}$ species will be enhanced with the increase in the basicity of surface O_s^{2-} ions. The latter supposition is confirmed by Mitchell, Sheinker, and White,[8] who showed that an introduction of sodium to high-purity γ-alumina increases the amount of chemisorbed sulfite by more than 10 times as compared to the undoped sample. Namely, the high Lewis basicity of CeO_2 provided a predominant contribution of strongly bonded sulfite species.[10] And at last, an enhanced concentration of hydrosulfite species should be observed in the case of the hydroxylated surface of high-surface area oxides.

The surface composition of the Al_2O_3 and CeO_2 films used in this study are determined by the procedure of their preparation. The UHV deposition of the corresponding metal followed by annealing in an O_2 atmosphere inside the spectrometer chamber suggests that we deal with high-purity, completely dehydroxylated surfaces of alumina and ceria with a low surface area. According to calculations of the electronic structure and energetics of the α-Al_2O_3 (0001) surface, the most stable configuration of the clean dehydroxylated sample is terminated by an Al layer,[40] which provides adsorption sites of the first type, Al_s^{3+}. This theoretically predicted structure was later experimentally confirmed by ion scattering spectroscopy (ISS) and reflection high-energy electron diffraction (RHEED).[41] At the same time, O^{2-} ions located in the second layer are also accessible, providing sites of the second type for SO_2 adsorption. Furthermore, the polycrystalline nature of our samples supposes that other planes, which are terminated by an oxygen layer, for example, $(1\bar{1}02)$,[40,42] can also be present on the surface. The accessibility of the Ce(IV) ions for adsorbates follows from recent data[43] obtained with the use of elevated-temperature STM. They have concluded that the unreduced CeO_2 (001) surface is stable if the oxygen coverage of the topmost layer is reduced to 50%.[43] The oxygen vacancies formed in this case provide the electroneutrality of the surface and the accessibility of Ce^{4+} ions located in the second layer.

These considerations allow us to propose a reasonable explanation of the above-mentioned experimental facts. The more efficient adsorption of SO_2 on the CeO_2 surface than that on the Al_2O_3 surface (Figures 1 and 2, Tables 2 and 3) is explained by the higher Lewis basicity strength of ceria as compared to alumina. Moreover, one can suggest that the low Lewis basicity of Al_2O_3 decreases considerably the concentration of chemisorbed SO_2 (bonded with O_s^{2-} ions) so that the contribution of physisorbed SO_2 (bonded with Al_s^{3+} ions) becomes predominant. This suggestion is supported by the suppression of the SO_2 adsorption in the presence of O_2 in the gas phase (compare Figures 1a and 2a). Note that a similar result was observed when water was coadsorbed with SO_2 (the spectra are not shown in this paper). Because both molecular oxygen and water are adsorbed on Lewis acid sites, only Al_s^{3+} ions, but not O_s^{2-} ones, were blocked in these experiments. As a consequence, one can suggest that the low intensive S2p features observed after the interaction of Al_2O_3 with the $SO_2 + O_2$ mixture at $T < 300$ °C (Figure 2a, Table 3) can be attributed to sulfite-like species adsorbed on O_s^{2-} ions, which are not affected by O_2 or H_2O adsorption. This could explain the small shift of the S2p lines to higher binding energies. A similar conclusion about the predominant contribution of the weakly bonded $SO_{2,ads}$ species on the alumina surface followed from data of Ziolek et al.,[10] who had shown that 71% of SO_2 is adsorbed reversibly on γ-Al_2O_3. Contrary to this, only 7% of adsorbed SO_2 could be desorbed from the CeO_2 surface.[10] At the same time, the above-discussed explanation of this shift in S2p binding energies due to admixing of sulfate formed in the presence of oxygen (see Results) cannot be avoided completely.

4.2. SO_4^{2-} Formation on Al_2O_3. The interaction of Al_2O_3 with pure SO_2 or with $SO_2 + O_2$ mixtures at temperatures above 300 °C results in the formation of sulfate-like species. This conclusion is based on the appearance of the $S2p_{3/2}$ feature at 169.1 ± 0.2 eV in the corresponding experiments (Figures 1 and 2). This implies that the process of sulfation is activated. The sulfate formation in the presence of molecular oxygen at high temperatures is well-known and has been reported many times.[2,3,6,8,11−14] Comparing the initial rates of adsorption and oxidative adsorption of SO_2, Nam and Gavalas[6] have shown that SO_2 adsorbed on the alumina surface can be oxidized to the sulfate ions

$$Al_2O_3 + 3SO_2 + {}^3/_2O_2 \rightarrow Al_2(SO_4)_3 \qquad (2)$$

which remain at the original SO_2 adsorption sites. Although aluminum sulfate is a thermodynamically stable compound, the authors did not observe the bulk sulfate phase in the IR spectra. They concluded that only surface sulfate could be produced at 350 °C and $P(SO_2) = 8$ mbar and $P(O_2) = 100$ mbar, that is, under the conditions similar to those used in our study. Based on IRS studies, the following sulfate structures on alumina surfaces were supposed.[11,17−19,44]

If the formation of surface aluminum sulfate via the reaction of the Al_2O_3 films with $SO_2 + O_2$ mixtures is expected (Figure 2), then the alumina sulfation under the influence of SO_2 in the absence of oxygen (Figure 1) looks strange. Indeed, the majority of the previous works, which have studied the adsorption of pure SO_2 on powdery alumina, have not reported the sulfate formation under comparable conditions.[2−8] To our knowledge, there was only one work where the reaction of SO_2 with γ-Al_2O_3 at 80 °C resulted in the parallel formation of sulfite and sulfate species characterized by the XPS $S2p_{3/2}$ lines with binding energies of 167.5 and 169.3 eV, respectively.[15] At the same time, the formation of the sulfate species was detected by XPS and XANES methods after small doses (several Langmuirs) of SO_2 adsorption on such nonreducible oxides as MgO and ZnO at room temperature or even below.[45−49]

Two mechanisms of the formation of sulfate species on the surfaces of alumina and other nonreducible oxides might be proposed. The first mechanism includes a disproportionation of sulfur dioxide into sulfate and SO species with a subsequent desorption into the gas phase[24,48]

$$Al_2O_3 + 6SO_2 \rightarrow Al_2(SO_4)_3 + 3SO \qquad (3)$$

However, evaluation of the thermodynamic parameters of this reaction for Al_2O_3 using the standard data tabulated in refs 50 and 51 leads to values $\Delta H_{298}^\circ \approx +29$ kJ/mol and $\Delta S_{298}^\circ \approx -635$ J/mol·K, which suggest that reaction 3 is hardly thermodynamically possible.

Another possible mechanism of the sulfation is based on an assumption that SO_4^{2-} surface species are formed upon the adsorption of SO_2 molecules on undersaturated oxygen ions,

the existence of which has been shown recently for the $(1\bar{1}02)$ surface by the crystal truncation rod (CTR) diffraction method.[42] It has been revealed that the most probable structure of this plane is terminated by additional oxygen ions situated above the theoretically predicted Al topmost layer. Such a kind of undersaturated oxygen species are less negatively charged as compared to usual O^{2-} anions in the bulk of alumina and, therefore, they could be sites for strong adsorption of SO_2 molecules in the form of the surface sulfate species. Assuming, for simplicity, that the undersaturated oxygen anions are singly charged, the sulfate formation could be described formally by the following reaction:

$$SO_2 + 2O_s^- \rightarrow SO_4^{2-} \quad (4)$$

It should be recalled that the polycrystalline structure of the alumina film prepared in this work allows a description of the surface by a set of different crystallographic faces separated by interplanar boundaries. The consequence of this mechanism of sulfation is the fact that the maximum possible sulfate yield cannot be equal to or exceed one monolayer. This conclusion is in agreement with the literature data that the amounts of sulfate species produced on alumina samples after their interaction with SO_2 even in the presence of oxygen were below 2×10^{14} atoms/cm^2.[7,10,13,16]

4.3. SO_4^{2-} Formation on CeO_2. The redox properties of CeO_2 make the sulfation of the CeO_2 surfaces under the reaction of ceria with pure SO_2 reasonable. The reduction of Ce(IV) ions to Ce(III) ones can be considered as a coupled semireaction, which provides the trapping of electrons that is necessary for the oxidation of SO_2 to surface sulfate or oxosulfate

$$6CeO_2 + 3SO_2 \rightarrow Ce_2(SO_4)_3 + 2Ce_2O_3 \{\text{or } 2CeO_2 + SO_2 \rightarrow Ce_2O_2(SO_4)\} \quad (5)$$

Indeed, the shift of S2p features to higher binding energies was registered after the interaction of the CeO_2 films with SO_2 at $T \geq 300$ °C as compared to the features measured at lower temperatures (Figure 1). This observation indicates the activated formation of the sulfate ions. The formation of Ce(III) sulfate was reported earlier by Diwell et al.[20] after the treatment of CeO_2 with 1 vol % SO_2 in nitrogen at 550 °C. Parallel sulfate formation and ceria reduction under annealing of ceria surfaces with adsorbed SO_2 at 550 °C or above was also concluded recently from XPS data by Ferrizz and coauthors.[25] Another mechanism of the sulfate formation without reduction of the CeO_2 surface

$$CeO_2 + 4SO_2 \rightarrow 2SO + Ce(SO_4)_2 \quad (6)$$

has been proposed by Rodriguez et al., who have concluded from XPS data (S2p) the appearance of the sulfate ions after SO_2 adsorption (5 L) on the surface of a ceria film at ambient temperatures.[24] It should be noted, however, that mechanism 6 was not supported by an analysis of the Ce3d spectra. This analysis was made in the present paper. The spectra presented in Figure 4a demonstrate unambiguously that the reduction of Ce(IV) into Ce(III) occurs when the sulfation proceeds under the influence of SO_2 at temperatures ≥ 300 °C.

Even the presence of oxygen in the $SO_2 + O_2$ mixtures during sulfation, which decreases the temperature of sulfation and increases the sulfate yield, does not prevent the reduction of Ce(IV) ions to Ce(III) ones (Figure 4b). Moreover, a quantitative correlation between the sulfate yields and the fraction of the Ce(III) ions is observed (Figure 5). The atomic ratio of the sulfate ions to Ce(III) ions estimated from these data ranges from 1.3 to 1.6, which is very close to the stoichiometric ratio of the Ce(III) sulfate (3:2). As a consequence, the sulfation in the presence of O_2 can be described formally by the following reaction:

$$2CeO_2 + O_2 + 3SO_2 \rightarrow Ce_2(SO_4)_3 \quad (7)$$

In the presence of oxygen, continuous growth of the concentration of the sulfate ions with temperature (Figure 3) suggests that sulfation of the CeO_2 proceeds not only on the surface but also spreads in the bulk. Earlier, the formation of two types of Ce(III) sulfates (surface and bulk-like) has been reported by Waqif et al.,[22] who have studied the sulfation of CeO_2 samples with different textures by IRS. They have shown that the relative amount of each type of sulfate species and the temperature of their formation depend on a composition of the reaction mixture (SO_2 versus $SO_2 + O_2$) and on the texture of the samples.

5. Summary

The interaction of Al_2O_3 and CeO_2 thin films with sulfur dioxide at a partial pressure of 2.5 mbar and $T < 300$ °C leads to the formation of sulfite species. This process is more effective for the CeO_2 surface, which is explained by a higher Lewis basicity strength of ceria as compared to alumina. The low Lewis basicity of alumina decreases the concentration of chemisorbed sulfite species (bonded with O_s^{2-} ions) on the Al_2O_3 surface, and the contribution of physisorbed SO_2 (bonded with Al_s^{3+} ions) becomes predominant. The dual mechanism of SO_2 adsorption is confirmed by suppression of the sulfite species formation if the oxides interact with SO_2 in the presence of oxygen.

An increase in the reaction temperature to 300 °C results in the formation of sulfate species. The formation of the sulfate species is accompanied by the reduction of ceria to cerium (III) sulfate or oxosulfate. The formation of sulfate species on alumina might be presented as adsorption of SO_2 molecules on the undersaturated surface oxygen anions.

Addition of oxygen to SO_2 facilitates the sulfation. In the case of CeO_2, the formation of the sulfate ions is observed at a temperature 100 °C lower than that in the case of pure SO_2. Moreover, the addition of oxygen to SO_2 increases the yield of sulfate on CeO_2 by a factor of 1.5−2. At elevated temperatures, the sulfation of ceria in the presence of oxygen results in the beginning of the formation of a 3D phase of cerium (III) sulfate. The effect of oxygen on the sulfation of Al_2O_3 is essentially smaller.

Acknowledgment. V.I.B. gratefully acknowledges the Russian Science Support Foundation, grant for young talented scientists.

References and Notes

(1) Truex, T. J. *SAE Paper* **1999**, 1999-01-1543.
(2) Chang, C. C. *J. Catal.* **1978**, *53*, 374.
(3) Babaeva, M. A.; Tsyganenko, A. A.; Filimonov, V. N. *Kinet. Katal.* **1984**, *25*, 787 (in Russian).
(4) Karge, H. G.; Dalla Lana, I. G. *J. Phys. Chem.* **1984**, *88*, 1538.
(5) Datta, A.; Cavell, R. G.; Tower, R. W.; George, Z. M. *J. Phys. Chem.* **1985**, *89*, 443.
(6) Nam, S. W.; Gavalas, G. R. *Appl. Catal.* **1989**, *55*, 193.
(7) Waqif, M.; Saad, A. M.; Bensitel, M.; Bachelier, J.; Saur, O.; Lavalley, J. C. *J. Chem. Soc., Faraday Trans.* **1992**, *88*, 2931.
(8) Mitchell, M. B.; Sheinker, V. N.; White, M. G. *J. Phys. Chem.* **1996**, *100*, 7550.

(9) Saad, A. B. M.; Saur, O.; Wang, Y.; Tripp, C. P.; Morrow, B. A.; Lavalley, J. C. *J. Phys. Chem.* **1995**, *99*, 4620.
(10) Ziolek, M.; Kujawa, J.; Saur, O.; Aboulayt, A.; Lavalley, J. C. *J. Mol. Catal. A: Chem.* **1996**, *112*, 125.
(11) Saur, O.; Bensitel, M.; Saad, A. B. M.; Lavalley, J. C.; Tripp, C. P.; Morrow, B. A. *J. Catal.* **1986**, *90*, 104.
(12) Waqif, M.; Saur, O.; Lavalley, J. C.; Perathoner, S.; Centi, G. *J. Phys. Chem.* **1991**, *95*, 4051.
(13) Pieplu, A.; Saur, O.; Lavalley, J. C.; Pijolat, M.; Legendre, O. *J. Catal*. **1996**, *159*, 394.
(14) Uy, D.; Dubkov, A.; Graham, G. W.; Weber, W. H. *Catal. Lett.* **2000**, *68*, 25.
(15) Gergely, B.; Guimon, C.; Gervasini, A.; Auroux, A. *Surf. Interface Anal.* **2000**, *30*, 61.
(16) Dalla Lana, I. G.; Karge, H. G.; George, Z. M. *J. Phys. Chem.* **1993**, *97*, 8005.
(17) Dosumov, K.; Umbetkaliev, A. K.; Popova, N. M. *Zh. Prikl. Khim.* **1994**, *67*, 1961 (in Russian).
(18) Dunn, J. P.; Jehng, J. M.; Kim, D. S.; Briand, L. E.; Stenger, H. G.; Wachs, I. E. *J. Phys. Chem. B* **1998**, *102*, 6212.
(19) Khadjivanov, K.; Davydov, A. *Kinet. Katal.* **1988**, *29*, 398 (in Russian).
(20) Diwell, A. F.; Hallett, C.; Taylor, J. R. *SAE Paper* **1987**, 872163.
(21) Beck, D. D.; Krueger, M. H.; Monroe, D. R. *SAE Paper* **1991**, 910844.
(22) Waqif, M.; Bazin, P.; Saur, O.; Lavalley, J. C.; Blanchard, G.; Touret, O. *Appl. Catal. B* **1997**, *11*, 193.
(23) Overbury, S. H.; Mullins, D. R.; Huntley, D. R.; Kundakovic, Lj. *J. Phys. Chem. B* **1999**, *103*, 11308.
(24) Rodriguez, J. A.; Jirsak, T.; Freitag, A.; Hanson, J. C.; Larese, J. Z.; Chaturvedi, S. *Catal. Lett.* **1999**, *62*, 113.
(25) Ferrizz, M.; Gorte, R. J.; Vohs, J. M. *Catal. Lett.* **2002**, *82*, 123.
(26) Kaichev, V. V.; Sorokin, A. M.; Timoshin, A. I.; Vovk, E. I. *Instrum. Exp. Tech.* **2002**, *45*, 58.
(27) Romeo, M.; Bak, K.; El Fallah, J.; Le Normand, F.; Hilaire, L. *Surf. Interface Anal.* **1993**, *20*, 508.
(28) Park, P. W.; Ledford, J. S. *Langmuir* **1996**, *12*, 1794.
(29) Moulder, J. F.; Stickle, W. F.; Sobol, P. E.; Bomben, K. D. *Handbook of X-ray Photoelectron Spectroscopy*; Perkin-Elmer: Eden Prairie, MN, 1992.
(30) Lindberg, B. J.; Hamrin, K.; Johansson, G.; Gelius, U.; Fahlmann, A.; Nordling, C.; Siegbahn, K. *Phys. Scr.* **1970**, *1*, 286.
(31) Visser, J. P. R.; Groot, C. K.; van Oers, E. M.; de Beer, V. H. J.; Prins, R. *Bull. Soc. Chim. Belg.* **1984**, *93*, 813.
(32) Brion, D. *Appl. Surf. Sci.* **1980**, *5*, 133.
(33) Manocha, A. S.; Park, R. L. *Appl. Surf. Sci.* **1977**, *1*, 129.
(34) Burroughs, P.; Hamnett, A.; Orchard, A. F.; Thornton, G. *J. Chem. Soc., Dalton Trans.* **1976**, 1686.
(35) Fujimori, A. *Phys. Rev. B* **1983**, *28*, 2281.
(36) Shyu, J. Z.; Weber, W. H.; Gandhi, H. S. *J. Phys. Chem.* **1988**, *92*, 4964.
(37) Shyu, J. Z.; Otto, K.; Watkins, W. L. H.; Graham, G. W.; Belitz, R. K.; Gandhi, H. S. *J. Catal.* **1988**, *114*, 23.
(38) Shyu, J. Z.; Otto, K. *J. Catal.* **1989**, *115*, 16.
(39) Paparazzo, E. *Surf. Sci.* **1990**, *234*, L253.
(40) Guo, J.; Ellis, D. E.; Lam, D. J. *Phys. Rev. B* **1992**, *45*, 13647.
(41) Suzuki, T.; Hishita, S.; Oyoshi, K.; Souda, R. *Surf. Sci.* **1999**, *437*, 289.
(42) Trainor, T. P.; Eng, P. J.; Brown, G. E.; Robinson, I. K.; De Santis, M. *Surf. Sci.* **2002** *496*, 238.
(43) Nörenberg, H.; Harding, J. H. *Surf. Sci.* **2001**, *477*, 17.
(44) Bensitel, M.; Saur, O.; Lavalley, J. C.; Morrow, B. A. *Mater. Chem. Phys.* **1988**, *19*, 147.
(45) Chaturvedi, S.; Rodriguez, J. A.; Jirsak, T.; Hrbek, J. *J. Phys. Chem. B* **1998**, *102*, 7033.
(46) Rodriguez, J. A.; Jirsak, T.; Chaturvedi, S.; Kuhn, M. *Surf. Sci.* **1999**, *442*, 400.
(47) Rodriguez, J. A.; Jirsak, T.; Freitag, A.; Larese, J. Z.; Maiti, A. *J. Phys. Chem. B* **2000**, *104*, 7439.
(48) Rodriguez, J. A.; Jirsak, T.; Perez, M.; Chaturvedi, S.; Kuhn, M.; González, L.; Maiti, A. *J. Am. Chem. Soc.* **2000**, *122*, 12362.
(49) Rodriguez, J. A.; Pérez, M.; Jirsak, T.; González, L.; Maiti, A. *Surf. Sci.* **2001**, *477*, L279.
(50) *CRC Handbook of Chemistry and Physics*; Lide, D. R., Ed.; CRC Press: Boca Raton, FL, 1992−1993.
(51) *Thermodynamic Properties of Individual Substances*; Glushko, V. P., Ed.; Nauka: Moscow, 1978.